

# Spark-Induced Breakdown Spectroscopy: A New Technique for Monitoring Heavy Metals

A. J. R. HUNTER,\* S. J. DAVIS, L. G. PIPER, K. W. HOLTZCLAW,† and M. E. FRASER‡

*Physical Sciences Inc., 20 New England Business Center, Andover, Massachusetts 01810*

This paper presents the development and testing of a new real-time monitoring technique for heavy metal aerosols and particulates in air based on spark-induced breakdown spectroscopy (SIBS). The technique is based on temporally resolved atomic emission resulting from excitation of the aerosol-laden air sample in a high-energy electrically generated spark. A complete prototype monitor comprised of spark power supply, sample chamber, bandpass-filtered radiometric detector, and computer for real-time data acquisition and display has been assembled, calibrated, and tested. The lower limits of detection for lead and chromium are  $10 \mu\text{g}/\text{m}^3$ . The monitor has been successfully applied as a continuous emissions monitor for lead and chromium in a simulated combustion flue gas at a joint EPA/DOE test, for fugitive chromium emissions above a hard chrome plating tank, and for airborne particulate lead at an indoor firing range. The monitor has also demonstrated the capability to detect cadmium, mercury, selenium, antimony, arsenic, uranium, and thorium.

Index Headings: Spark-induced breakdown spectroscopy; SIBS; Heavy metal monitoring; Atomic emission; Continuous emissions monitor.

## INTRODUCTION

Sensitive, real-time monitors for airborne heavy metals have applications in environmental compliance and industrial hygiene. Two of the most serious heavy metal exposure hazards in the workplace are lead and chromium. OSHA (Occupational Safety and Health Association) has estimated that nearly 1 million U.S. construction workers are exposed to lead with the most severe exposures occurring to the 50 000 to 60 000 workers involved in the rehabilitation of highway and railroad bridges and large tanks.<sup>1,2</sup> In addition to the construction industry,<sup>3</sup> significant occupational exposures to lead occur in primary and secondary lead production;<sup>4</sup> the manufacture of brass, bronze, copper, and other non-ferrous metals; the electronics industry; lead acid battery manufacture; automobile radiator repair shops; the manufacture of ink, paints, wall paper, and cans;<sup>5,6</sup> and indoor gun firing ranges,<sup>7-9</sup> of which there are several thousand in the U.S.

Exposure to chromium is a known hazard associated with hard chromium electroplating,<sup>10-14</sup> abrasive blasting of painted surfaces,<sup>15,16</sup> cement working,<sup>11</sup> and stainless steel welding.<sup>12</sup> The recognition of hexavalent chromium, Cr(VI), as a carcinogen, and therefore as one of the most toxic of the 189 hazardous air pollutants, has caused the

EPA (Environmental Protection Agency) and OSHA to place severe restrictions on atmospheric release and worker exposure to fugitive emissions of this species, respectively. The EPA has set regulatory limits for new sources at  $15 \mu\text{g}/\text{dscm}$  (dry standard cubic meter) and  $30 \mu\text{g}/\text{dscm}$  for existing sources. The current OSHA permissible exposure level (PEL: permissible exposure level, ceiling) for chromic acid and chromates is  $100 \mu\text{g}/\text{m}^3$  and the National Institute for Occupational Safety and Health (NIOSH) REL [recommended exposure level; 10 h TWA (time-weighted average)] is  $1 \mu\text{g}/\text{m}^3$ . OSHA is currently considering a revision of the PEL to an 8 h TWA for Cr(VI) at a level of  $0.5 \mu\text{g}/\text{m}^3$  with an action level of  $0.25 \mu\text{g}/\text{m}^3$ .

For environmental compliance, implementation of the 1990 Clean Air Act will require monitoring of several toxic metals in combustion flue gases. These metals are beryllium, arsenic, chromium, cadmium, lead, and mercury. Both workplace hygiene and stack monitoring for airborne heavy metals have historically been accomplished by sample extraction and laboratory analysis with the use of inductively coupled plasmas (ICP) or atomic absorption spectrometry (AAS). The sampling procedure is typically performed over one or more hours, and the laboratory results returned within one to two weeks. This procedure is unacceptable for environmental compliance as the metals concentrations in stack gases can be highly variable. Thus, this application requires a continuous emissions monitor (CEM) capable of providing accurate metals concentration measurements in real time and at fine time scales (2 min). Many industrial settings have similar monitoring needs to effectively limit and control worker heavy metal exposure.

This paper describes the development and performance results for the spark-induced breakdown spectroscopy (SIBS) technology. SIBS is a newly developed *in situ* measurement technique based on atomic emission resulting from a high energy (typically 5 J) spark.<sup>17</sup> It has been developed to perform sensitive, real-time monitoring of airborne metals for both environmental compliance and industrial hygiene applications.

## DISCUSSION

**Basis of Spark-Induced Breakdown Spectroscopy.** SIBS is fundamentally an atomic emission spectroscopic technique requiring a method of spark formation, an optical detection method, and a sampling scheme. In the case of the SIBS applications described herein, these functions are performed with an electric spark power supply, either wavelength-dispersed or radiometric detection,

Received 8 February 1999; accepted 24 November 1999.

\* Author to whom correspondence should be sent.

† Current address: Micron Technology, Inc., 8000 S. Federal Way, Boise, ID 83707.

‡ Current address: Mission Research Corporation, One Tara Boulevard, Suite 302 Nashua, NH 03062.

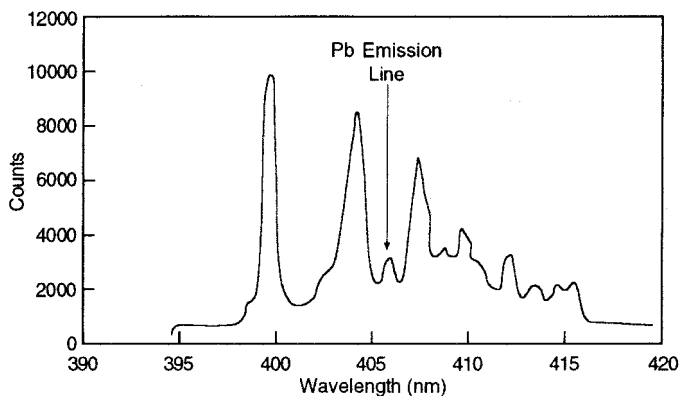


FIG. 1. SIBS spectrum of Pb aerosol with no delay between spark and detection.

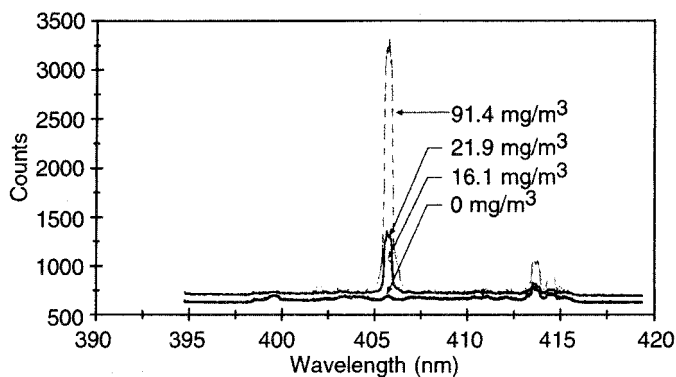


FIG. 2. SIBS spectra in the region of 406 nm at different Pb-aerosol concentrations with detection delayed 75  $\mu$ s after the excitation spark.

and an electrode and sampling assembly suitable for calibration and contaminated air sampling.

The spark power supply contains an EG&G power supply (<2000 V, 100 J/s) integrated with a capacitor bank. After the capacitors are charged, a trigger pulse initiates the creation of an ion channel between the electrodes through a high-voltage (40 kV), low-current pulse provided by an automotive ignition coil. This channel creates a low resistance path for the prompt discharge of the capacitor bank. The total discharge energy can be varied from 1 to 5 J with <0.5 J arising from the initiator pulse. The spark frequency was generally operated at 1 Hz with frequencies up to 10 Hz permitted by the power supply. A safety interlock system has been incorporated into the power supply to prevent accidental high-voltage exposure.

In both LIBS (laser-induced breakdown spectroscopy) and SIBS, the light emitted from the spark is utilized to identify the species present. The discharge heats the air between the electrodes to extremely high temperatures (in excess of 5000 K<sup>18</sup>). The air and any particles are vaporized and ionized, resulting in a plasma of ions and electrons.

The spark occurs between two separated electrodes (typical gap is 5 to 6 mm) that have been placed at the centerline of the sampled gas flow. The electrodes are composed of a proprietary material chosen for high corrosion resistance, high melting temperature, and low ablation propensity. The electrode material has also been chosen to be free of spectral interferences in the chosen radiometer bandpasses.

The electrode gap currently employed is the largest that enables reproducible sparking and has been maximized to improve sensitivity. At low concentrations in the region of regulated levels (on the order of 50  $\mu$ g/m<sup>3</sup>) the number of particles per cm<sup>3</sup> falls below 100 even for submicrometer particle sizes. Thus, techniques such as LIBS that process very small volumes (Radziemski and Cremers<sup>19</sup> report the spark volume from a 100 mJ Nd:Yag laser to be 0.003 cm<sup>3</sup>) typically employ a conditional sampling approach to select the 2 to 5% of the shots that actually process a particle. Because of a greater sampling volume (0.1 cm<sup>3</sup>), the SIBS technique needs only multiple shot averaging to achieve acceptable reproducibility (60 to 120 sparks are typical for low concentrations).

The character of the light emitted in the breakdown region depends upon the delay after spark ignition. At times immediately after ignition (a few microseconds) the radiation is a spectral continuum characteristic of the emission of hot free electrons with little additional spectral structure, as shown in Fig. 1. As the plasma cools, structured emission becomes more prominent that is characteristic of the species with high internal energy, principally ionized atoms. Continued cooling results in recombination of the ions with electrons and produces species of lower energy that then emit light at their own characteristic frequencies. For these reasons, the spectra tend to become less complex at long times (>20  $\mu$ s) after ignition, as shown in Fig. 2. Typical delay times of 20 to 50  $\mu$ s are used to gate past the bright continuum radiation due to plasma recombination and detect the more persistent atomic emission of the analyte metals.

Optical detection has been performed by using lenses or optical fibers (600  $\mu$ m diameter, multi-mode) with spectrometer/optical multichannel analyzer (OMA) combinations and optical fibers with interference-filtered radiometers. The OMA system was used to perform spectral surveys and interference studies and the radiometers used to optimize quantitative detection of single analyte metals. The spectrometer/OMA system was composed of a 0.32 m focal length monochromator (2400 grooves/mm grating, blazed at 250 nm) with a pulsed optical multichannel analyzer (Princeton Instruments) having an intensified linear diode array. Good signal-to-noise could be achieved with accumulation times of about 10 s. A photodiode and second delay generator were used to trigger the OMA to avoid saturation from the bright initial plasma.

Two radiometer detectors have been constructed for the quantitative monitoring of lead and chromium, respectively. Each of these units is composed of two miniaturized photomultiplier tubes (PMTs) (Hamamatsu) and two interference filters [1 nm full width at half-maximum (FWHM), Andover Corporation]. One filtered PMT collects the emission from the atomic line (for example, 405.7 nm for Pb) and the other filter collects light from a wavelength region containing only residual plasma emission (400 nm was chosen for lead detection). Figure 3 demonstrates this approach, showing the spectrum obtained from the spark-discharge of a lead-containing aerosol, superimposed with the transmission curves of the

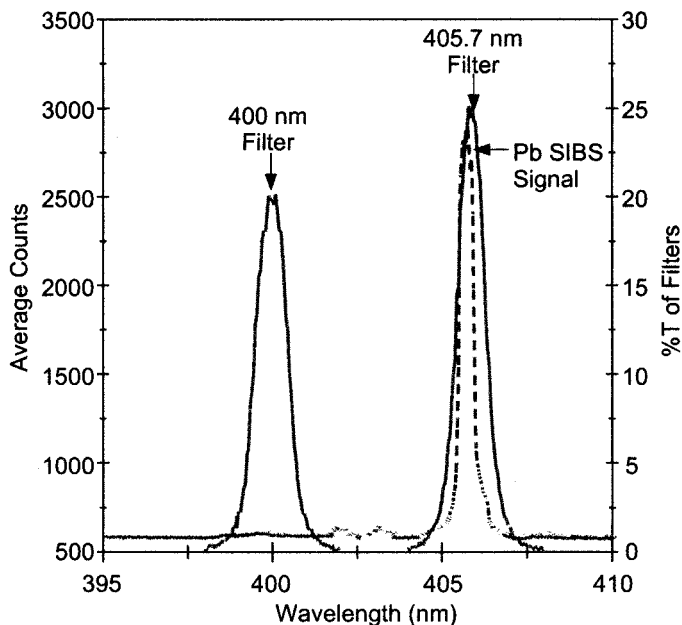


FIG. 3. Transmission curves of the detection filters superimposed on SIBS-acquired lead emission spectrum.

two filters. For chromium, the analyte atomic line was chosen to be 427.5 nm with 420 nm selected for background. For all three monitoring applications described in this paper, these spectral regions were determined to be free of spectral interferences in tests using representative samples at the anticipated relative concentrations.

The radiometer analog voltage output signals are input into a 1.2 MHz A/D data acquisition board (National Instruments) mounted in a PC and are finally converted into an on-screen strip chart display of concentrations through the use of an in-house developed program based on Lab Windows CVI® software. This system subtracts the temporally coincident background signals from the analyte atomic line data, which allows selection of the optimal delay and integration period for sensitive detection. The program also includes various user-input settings for averaging and data saving.

Finally, the SIBS system requires an electrode and sampling assembly to house the electrodes and fiber optics and to provide an interface to the application. In order to measure metals *in situ* in a waste incinerator duct, a probe (Fig. 4) was designed to support the electrodes at the duct centerline. The electrodes were mounted on ceramic standoffs and were oriented normal to the gas flow so that flow through the gap was unimpeded. The probe is entirely enclosed (stainless steel front and rear plates with an aluminum body), with a quartz window to pass the spark emission to a bundle of six optical fibers (400 μm diameter, high-temperature compatible), which terminated in SMA connectors on the rear of the probe. Another bundle of optical fibers (600 μm diameter, 10 m long) transmitted the light to the radiometers. During use in the high-temperature (230 °C) conditions, the probe was air cooled from the rear with the exhaust through the front plate into the duct.

The probe was adapted for calibration testing and for ambient air monitoring with the use of an acrylic plastic housing and stand and a small pump (0.028 m<sup>3</sup>/min) to

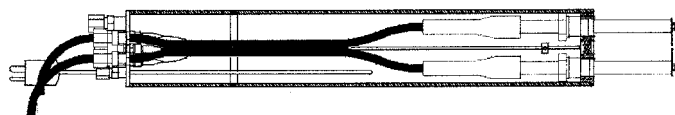


FIG. 4. SIBS probe design.

draw the sample stream through the electrode gap. This scheme is demonstrated in Fig. 5. An advantage of this simple gas handling system is that a filter can be placed between the spark gap and the pump to allow correlations between the SIBS data and filter samples that were analyzed by digestion and atomic absorption or ICP spectrometry by an independent laboratory.

**Dry Aerosol Calibration System.** Metal-containing aerosols to calibrate and characterize instrument response were produced with the use of droplet generators coupled to a drying column. One droplet generator is a variant on the design demonstrated by Berglund and Liu.<sup>20</sup> Similar systems have been employed by other researchers (see, for example, Zynger and Crouch<sup>18</sup>). The operating principle involves the imposition of a periodic instability on a thin stream of fluid flowing from a pinhole orifice. The instability is induced by coupling a single-frequency vibration into the fluid by using a piezoelectric transducer driven by a square wave function generator. Under certain conditions of fluid flow rate and instability frequency, monodisperse aerosols are generated.

The size of the droplet is a function of the instability frequency and fluid flow rate through the orifice:

$$D_p = \left( \frac{6Q}{\pi f} \right)^{1/3} \quad (1)$$

where  $Q$  is the fluid flow and  $f$  is the frequency. A frequency of 100 kHz, a flow rate of 0.34 mL/min, and an orifice size of 20 μm were used to produce droplets 48 μm in diameter.

The droplet generator is situated at the top of a Plexiglas tube in a downward-directed orientation toward the

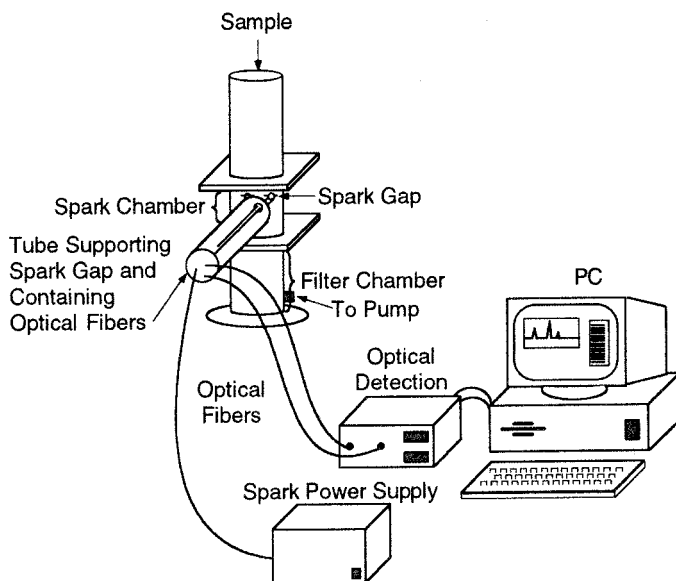


FIG. 5. Schematic diagram of prototype industrial hygiene monitor (not to scale).

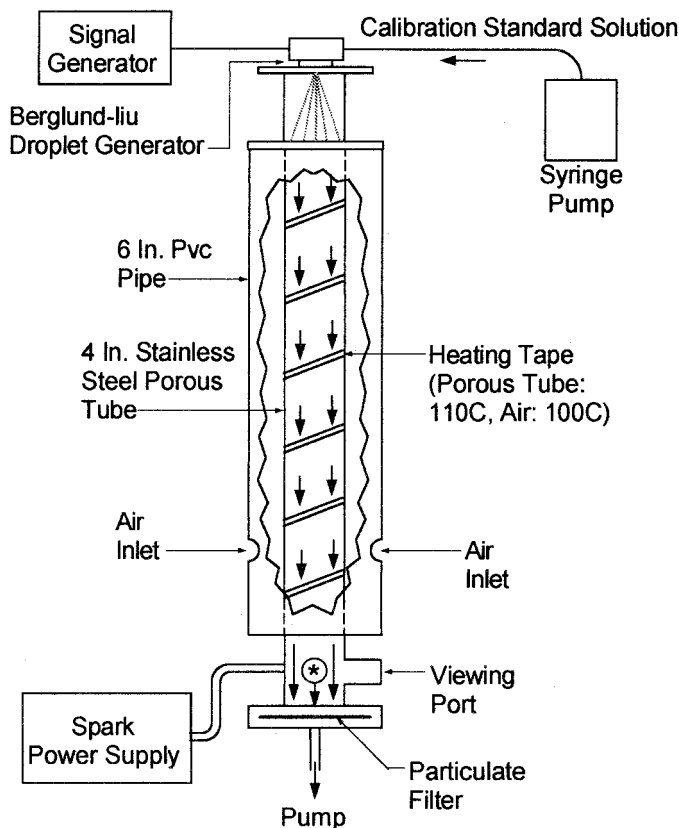


FIG. 6. The dry aerosol source, including spark chamber and drying tube.

drying column (Fig. 6). Loss of particles on the drying column walls is minimized by using a porous, stainless steel inner tube through which air is drawn at a fixed rate. The flow rate ( $0.028 \text{ m}^3/\text{min}$ ) has been chosen to provide a gas flow rate that exceeds the particle terminal velocities. The air is heated to  $110^\circ\text{C}$  to facilitate removal of water from the droplets and is drawn out the bottom of the column by a filtered pumping system. The dry aerosol ( $0.3$  to  $3 \mu\text{m}$  diam) is trapped on a filter placed at the bottom of a Plexiglas extension under the drying column that houses the spark chamber. This filter prevents particles from exiting the generator and contaminating the air pump.

In order to calculate the concentration of aerosol, the efficiency with which the aerosol traverses the drying tube needs to be accurately measured:

$$C_{\mu\text{g}/\text{m}^3} = \frac{M(\mu\text{g}/\text{min}) \cdot E}{F(\text{m}^3/\text{min})} \quad (2)$$

Here,  $M$  is the mass introduction rate,  $E$  is the passage efficiency (particle loss in the generator), and  $F$  is the air flow. The aerosol concentration is changed by varying the input solution concentrations.

The dry aerosol generator has been calibrated gravimetrically by comparing the input aerosol mass flow rate to the mass recovered on a filter at the bottom of the drying tube. This defines the passage efficiency,  $E$ , of the aerosol particles in the calibration system. The gravimetric procedure uses a high-flow filter with a nominal pore size of  $1 \mu\text{m}$  that was dried in an oven at  $160^\circ\text{C}$  for

TABLE I. Results of aerosol mass recovery tests.

Solution concentration (% wt)	Mass recovery efficiency	Dry particle diameter ( $\mu\text{m}$ )	Lead concentration ( $\text{mg}/\text{m}^3$ in air)
0.091	0.95	4.6	10.3
0.41	0.90	7.6	43.4
0.41	0.88	7.6	43.0
0.93	0.85	10	94.1

about half an hour to remove any absorbed water. The filter was then weighed and introduced into the aerosol generator without the spark chamber, and one of several high-concentration solutions of lead nitrate was fed through the droplet generator. The solutions are prepared from National Institute of Standards and Technology (NIST)-traceable ICP standards. High concentrations (in the  $\text{mg}/\text{m}^3$  range) are used for this gravimetric analysis to generate enough mass on the filters to be easily differentiated from the preweight. After a prespecified time the filter was removed and heated again to  $160^\circ\text{C}$  for half an hour (since the column beneath the droplet generator was heated to  $110^\circ\text{C}$ , there was probably not any water remaining, but this step ensured that each filter was in the same dry state, before and after). Following the final drying step, the filter was weighed again. The mass difference was then compared with the known amount of metal salt introduced into the generator. The mass recoveries (passage efficiencies) are uniformly high (0.85 to 0.95), indicating that particle losses within the generator/drying tube are minimal. Table I displays the results of the mass recoveries and the calculations of dry particle diameter and lead concentration. Passage efficiencies of the smaller particles used in the lower portion of the calibration curve will be similar, as their smaller size will allow even more efficient entrainment into the gas flow.

In addition to the Berglund-Liu droplet generator, a commercial package from Sonotek has also been employed. This device was chosen for greater reliability and ease of use. The Sonotek system was also gravimetrically verified to deliver 80 to 95% of the particles to the filter. The Sonotek unit generated polydisperse droplets ultrasonically with a narrow distribution centered at  $18 \mu\text{m}$  in diameter.

The commercial Sonotek units are sufficiently rugged to allow portable field calibration systems to be constructed. For some applications, such as stack gas monitoring, *in situ* calibration (direct injection of calibration standards into the stack) is needed due to the elevated temperatures, high moisture content, and sample complexity. Even extractive techniques containing an internal calibration procedure would benefit from such a system to quantify sampling losses.

**Calibration.** The SIBS instrument has been calibrated for lead and chromium aerosols over the  $0$  to  $10\,000 \mu\text{g}/\text{m}^3$  range. The detection limits have been determined following the procedure outlined in Appendix 3 of the NIOSH publication "Guidelines for Air Sampling and Analytical Method Development and Evaluation".<sup>21</sup> The guide recommends five or more standards up to two times the regulated level ( $50 \mu\text{g}/\text{m}^3$  for lead). The calibration system was used to create air concentrations of lead nitrate aerosol particles in the range  $0$  to  $81.2 \mu\text{g}/\text{m}^3$ . The

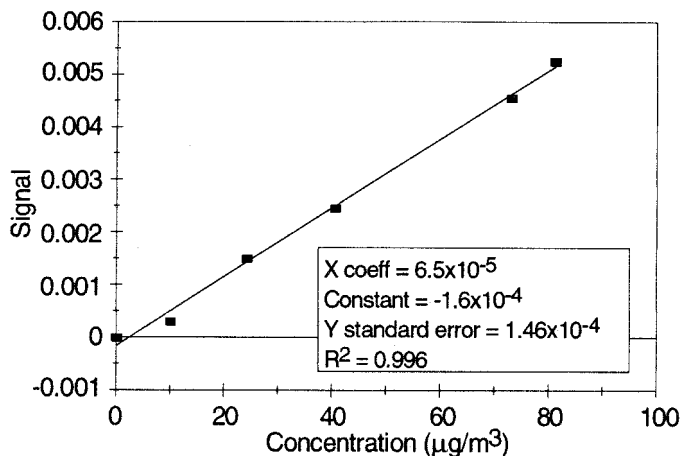


FIG. 7. Lead calibration curve.

resulting calibration curve with best-fit line is shown in Fig. 7. As recommended by the guide, these data have been used to determine the standard error of the regression,  $\sigma_y$ , the slope,  $m$ , and the linear fit constant,  $b$ . The lower limit of detection (LOD) defined by the guide is provided by  $\text{LOD} = 3\sigma_y/m = 6.7 \mu\text{g}/\text{m}^3$ .

However, the guide specifies that the reported LOD be the highest of (1) calculated LOD, (2) lowest calibration standard, or (3) X-intercept. For these data the lowest calibration standard,  $10 \mu\text{g}/\text{m}^3$ , is the highest value so this is the reported LOD. The limit of quantitation (LOQ), which is the smallest concentration of analyte that can be measured with precision, is then calculated from the guide,  $\text{LOQ} = 3.33 \times \text{LOD} = 33 \mu\text{g}/\text{m}^3$ . A similar procedure for chromium produced a value of  $10 \mu\text{g}/\text{m}^3$  for the LOD.

**Interference Measurements.** The most likely interference in SIBS is spectral overlap. This overlap could occur from other elements in the sample or from the electrodes themselves. The 405.7 nm Pb atomic line and 400 nm background wavelengths were initially chosen because they were suitably free from electrode lines. In a procedure to verify that the lines for lead and chromium were free from interferences in a stack gas environment, stack gas-equivalent concentrations ( $>1000 \mu\text{g}/\text{m}^3$ ) of iron, aluminum, silica, calcium, and magnesium (these are the principal ash components<sup>22,23</sup>) were generated and sampled. Spectrally resolved data were then taken with the spectrometer/OMA combination. The results indicated there to be no spectral interferences from these elements in any of the wavelength regions at the bandwidth (1 nm FWHM) of the radiometer filters. The potential spectral interferences in a lead paint abatement application have also been examined, and the lead line has been determined to have no spectral overlap with typical inorganic paint components—aluminum, manganese, iron, and titanium.

**Speciation.** In an effort to examine lead speciation effects, aerosols of identical concentrations ( $442 \mu\text{g}/\text{m}^3$ ) of lead(II) chloride, lead(II) nitrate, and lead(II) acetate were generated. These aerosols were introduced sequentially into the spark chamber, allowing the signal to return to near baseline among additions. These data showed no distinction between the three types of lead species.

TABLE II. Metals examined with SIBS.

Metal	Estimated limit of detection ( $\mu\text{g}/\text{m}^3$ )
Pb	$10^a$
Cr	$10^a$
Hg	$<40$
Cd	$<120$
U	$<400$
Th	$<1200$

<sup>a</sup> Measured  $3\sigma$  lower limit of detection using radiometer.

Equivalent response to lead oxide has also been demonstrated.

ICP standards of chromium(III) nitrate, chromium(VI) nitrate, and chromium(VI) chloride were also tested. The calibration curve encompassed seven points over the range 0 to  $1500 \mu\text{g}/\text{m}^3$ . Identical sensitivities were observed for all three compounds. The insensitivity of the observed SIBS response to the various chemical forms tested is believed to be due to the high spark plasma temperatures. Further work on speciation (water-insoluble compounds), matrix effects, and interferences is in progress.

**Extension to Other Metals.** In addition to lead and chromium, the SIBS device is capable of detecting other elements provided that a suitable interference-free wavelength can be found. With the use of the multichannel analyzer, suitable wavelengths for the detection of mercury, cadmium, uranium, and thorium have been located in the near-UV to visible region, and calibration curves for these species have been determined over the 0 to  $>1000 \mu\text{g}/\text{m}^3$  concentration range. From the signal-to-noise limits on the multichannel analyzer, estimates of the lower limit of detection have been derived. The results are shown in Table II. The values are shown as upper limits as the detection limits optimized by using the band-pass filtered-radiometer have generally been found to significantly improve those from the multichannel analyzer. The results for cadmium and mercury are promising, but reduction of the LOD to  $<10 \mu\text{g}/\text{m}^3$  will be necessary for ambient monitoring of these two species. Mercury will be particularly challenging as this species is often distributed in both the gas and condensed phases in many monitoring applications (vapor-phase mercury and solid mercuric chloride are encountered in combustion flue gases with the former generally dominant under most conditions).

Uranium and thorium were tested, as the longer-lived radioisotopes of these elements are frequently encountered in site cleanups of Department of Energy (DOE) hazardous waste sites. Weaker atomic emission lines are principally responsible for the reduced LODs of these species. The results for these two species indicate that unambiguous identification of these two elements can be achieved, but further optimization of the LODs will be needed for a survey instrument to meet regulatory limits [American Conference of Governmental Industrial Hygienists (ACGIH) limit for the inhalation of insoluble  $\text{U}^{238}$  is  $\sim 600 \mu\text{g}/\text{m}^3$ ].

**Instrument Use.** The SIBS spark samples the aerosol-containing air between the two electrodes. In an application the contaminated air can be actively drawn through

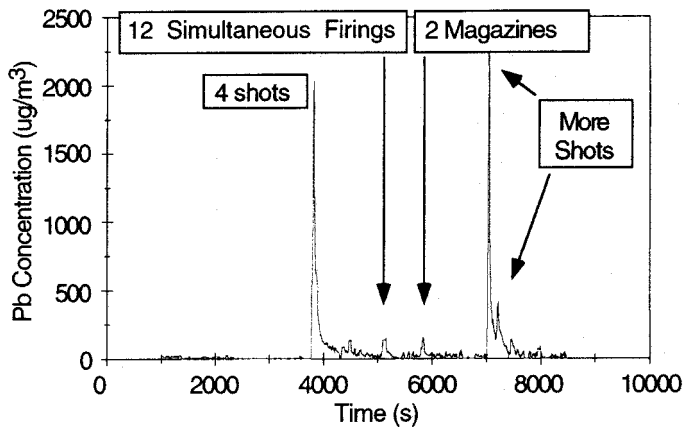


FIG. 8. Linear plot of firing range data.

the electrodes by a pump or the spark can passively sample an active flow, as in an exhaust duct.

The fielded systems for both ambient air monitoring and stack gas monitoring are modular and require less than an hour to connect and interface to the application. The unit currently relies upon calibration performed in the laboratory immediately before shipment. Empirically it has been determined that the calibrations will hold to  $\pm 5\%$  as long as electrode alignment is maintained. Occasionally, the electrodes become misaligned during shipment; they are easily repositioned with the use of a small diode laser directed through the optical fibers through the electrode gap onto a template that represents optimal alignment. Re-adjustment of the electrodes is not common and is generally necessary only after physical mishandling of the probe.

Reliable, reproducible sparking is generally obtained in ordinary room air and in humidified air at elevated temperature. Occasionally, the unit will miss sparks in dry air. We are considering simple engineering solutions for this problem, such as prehumidification of the sampled air.

Very little routine maintenance of the instrument is needed. When exposed to high concentrations of analyte, the Plexiglass body for the ambient air monitoring application must be removed and cleaned, and the elec-

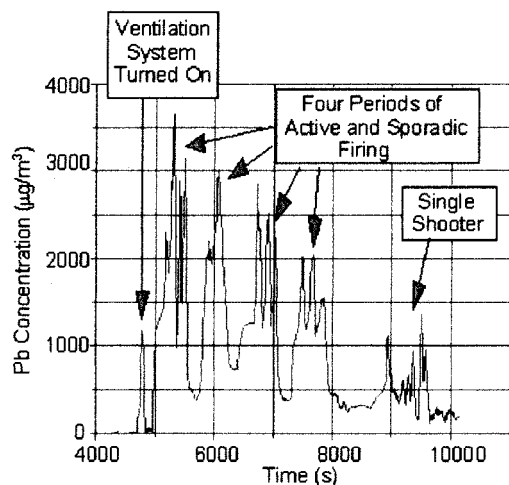


FIG. 9. Crawl space lead data.

trodes must be cleaned. The procedure for cleaning the electrodes is to swab them sequentially with dilute nitric acid, water, and then methanol. If extremely high concentrations of analyte have been encountered, it is sometimes necessary to gently sand the electrodes with a fine-grit sandpaper to remove residual analyte material. The typical time for this procedure is about 10 min.

**SIBS Applications and Field Tests.** *Lead at an Indoor Firing Range.* Two field tests of the instrument were performed at a nearby firing range. The range is a state-of-the-art facility with clean air introduced behind the shooting booths. The air flow entrains the lead and carries it away from the shooters downrange through a ventilation system and into a set of high-efficiency particulate air (HEPA) filters.

For the first test the lead monitor was placed immediately in front of one of the firing booths (total of 20 booths). Active handgun firing was occurring 10 ft away. For these tests 15 booths (shooter locations) were active.

Quantitative data from this test are shown in Fig. 8. The vast majority of the data show the measured lead concentration to be at or near the detection limit of  $10 \mu\text{g}/\text{m}^3$ , well below the OSHA regulated level of  $50 \mu\text{g}/\text{m}^3$ . Only six events were recorded showing the lead concentration exceeding  $100 \mu\text{g}/\text{m}^3$ . The majority of these, however, were when firing occurred directly over the sample inlet. The first of these occurred near 3900 s when four revolver rounds were fired. The ammunition was a conventional type. The second event is near 5900 s when two full magazines from a semiautomatic pistol were fired overhead. Finally, in the time 7000 to 7300 s two different weapons were fired.

In the time period 6000 to 7000 s, ammunition specifically manufactured to be lead free was tested. No significant lead readings were obtained when the ammunition was discharged directly over the sample inlet. Of the remaining events, at 5100 s approximately 12 individuals simultaneously fired two or more clips consecutively, and that smoke could be visually detected at the sampling location.

This carefully designed state-of-the-art range is extraordinarily clean and free of lead contamination. However, other firing ranges, particularly those of older construction and in private use, often have ambient airborne lead levels approaching  $2000 \mu\text{g}/\text{m}^3$ . The time-weighted average of lead data for the test period was  $54.3 \mu\text{g}/\text{m}^3$ , which is above the regulated  $50 \mu\text{g}/\text{m}^3$  limit. However, it is important to note that this level is an extreme exposure upper limit, as the majority of the data was deliberately introduced by firing above the instrument inlet, which is not representative of the shooter's airspace. Even with this caveat, however, an 8 h TWA of the data works out to  $13.5 \mu\text{g}/\text{m}^3$ —well below the action level, since the test period was the only activity that day.

A second test was performed at this range. For this entry, the lead monitor was placed downrange in the ventilation crawl space immediately before the contaminated air passed through the filters. The data are shown in Fig. 9. All the data before 4000 s have been excluded, because this was before any firing was occurring and there was no measurable lead.

The spike in lead just before 5000 s was caused by the ventilation system being turned on. No firing took place,

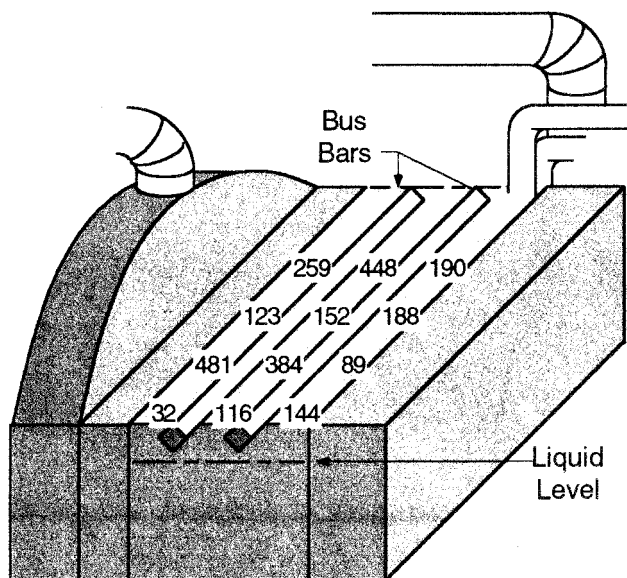


FIG. 10. Plating tank sampling locations and measured chromium concentrations in  $\mu\text{g}/\text{m}^3$ .

but the turbulent airflow stirred up lead particulate in the ventilation room, producing a signal.

When active firing took place, the concentration reached as high as  $3000 \mu\text{g}/\text{m}^3$  in the ventilation room. This range, of course, reaches this level only in the ventilation crawl space just before the filters. The airborne lead and lead oxide are carried by the air flow from the shooting positions to the HEPA filters consistent with the data obtained with the SIBS monitor.

The data show four separate active periods of firing, each with spikes corresponding to different levels of activity. During the test each of the enhanced lead concentration spikes correlated well with periods of firing. During the inactive periods the concentration always decreased. The TWA exposure data for Fig. 10 are  $950 \mu\text{g}/\text{m}^3$  for the test period and  $178 \mu\text{g}/\text{m}^3$  for 8 h. This latter value is well above the regulated limit and supports the decision of the range designer to provide access to the crawl space only through a sealed panel. Finally, at the end of the test the monitor detected the lead produced from a single shooter.

*Continuous Emissions Monitoring of Combustion Flue Gases.* The SIBS technology has been tested as a continuous emissions monitor. During the summer of 1997 the spark probe was adapted to mount into an 8 in. schedule 10 duct to monitor lead and chromium at the rotary kiln incinerator simulator (RKIS) at Research Triangle Park, NC.<sup>23,24</sup> This was a test co-sponsored by both EPA and DOE to identify continuous emissions monitors for resource conservation and recovery act (RCRA) metals monitoring under the proposed amendments to the 1990 Clean Air Act. SIBS was evaluated alongside other developing CEMs: inductively coupled plasma atomic emission spectroscopy (ICP-AES),<sup>25,26</sup> laser-induced breakdown spectroscopy,<sup>27</sup> and microwave plasma.<sup>28</sup> Two separate groups tested LIBS systems. The work of Singh et al. was reported in the EPA final document,<sup>23</sup> but their technology summary was omitted. Actual metal concen-

trations were measured during the tests by using EPA Reference Method 29.

The gas temperature at the SIBS sampling port was typically  $230 \text{ }^\circ\text{C}$  ( $450 \text{ }^\circ\text{F}$ ). The particle loading in the exhaust gas was  $30 \text{ mg}/\text{acm}$  (actual cubic meter), and the stack gas velocity was  $31 \text{ ft/s}$  ( $9.45 \text{ m/s}$ ). The average particle size was analyzed to be  $0.5 \mu\text{m}$ . There were no acid gases present, and typical  $\text{CO}_2$  and water concentrations were 2.9 and 7%, respectively.

The SIBS technology successfully detected both lead and chromium at the low- and high-level concentrations.<sup>23,29</sup> Additionally, the hardware performed without failure for  $>100 \text{ h}$  of operation and acquired data for 100% of the reference method tests. The chromium data were well correlated with concentration increases resulting from duct operations and pressure fluctuations that are known to entrain dust.

A total of six CEM developers, including SIBS, participated in this test. A principal conclusion of the EPA final test report<sup>23</sup> is that none of the technologies obtained data within the required 20% relative accuracy (RA) target. We have carefully re-analyzed the EPA reference method 29 data and have concluded that systematic reference method (RM) variabilities precluded meeting this benchmark and that relaxation of the RM goal to 50–75% would be a more reasonable target.<sup>29</sup>

*Fugitive Emissions above a Hard Chromium Plating Tank.* The instrument has also measured fugitive chromium emissions above a hard chromium electroplating tank.<sup>30</sup> The testing was performed side-by-side with OSHA Draft Method ID-215 (filter sampling). The goal of this test was to enable the plating facility to optimize its air handling system with no danger from increased fugitive chromium emissions.

The SIBS monitor acquired data on a 5 s time scale and was used to survey the total chromium concentrations above the plating bath surface during ventilation changes and other operations. The SIBS measured concentrations varied from  $<10 \mu\text{g}/\text{m}^3$  (the monitor detection limit) to  $>1000 \mu\text{g}/\text{m}^3$ . Sample results are shown in Fig. 10 with the concentration units in  $\mu\text{g}/\text{m}^3$ . The concentrations were determined at 17 in. above the plating bath surface with the ventilation system on. The measured concentrations were well correlated to distance from the plating bath surface, smoke test indicators of "hot spots," and ventilation flow rate.

The SIBS data quantitatively agree (to within 20%) with simultaneous internal filter results and with the OSHA air sampling filter measurements. These results indicate that the SIBS monitor is capable of performing industrial hygiene monitoring of chromium in a plating environment.

## CONCLUSION

The field tests have demonstrated that the SIBS instrument is capable of use as a continuous emissions monitor and as an industrial hygiene instrument. The current fielded system can fit on a tabletop or in a 19 in. rack, and the total component cost is low compared to the other alternatives, such as LIBS. The next development phase will be to incorporate the entire system into a single package easily transported by a single user in an industrial

hygiene application. Improvement in the LODs for lead and chromium will be made at the next developmental stage by blinding the photomultiplier tubes to the majority of the early time bright plasma, enabling higher gains to be used. The target for lead is 3 to 5  $\mu\text{g}/\text{m}^3$ , representing a factor of 10 difference between the regulated level and the LOD. Improvements for chromium detection to  $<1 \mu\text{g}/\text{m}^3$  will be sought to meet the NIOSH REL for Cr(VI). Sufficient data will be obtained with the new monitor to allow for NIOSH approval of the method<sup>32</sup> for industrial hygiene monitoring.

#### ACKNOWLEDGMENTS

The authors acknowledge support from DOE (under contract DE-AC21-93MC30175), DoD (under contract DACA88-95-C-0004), NIOSH (under SBIR Phase I grant IR430H03505-01), and PSI IRAD for contributing to the development of this technology.

1. Occupational Safety and Health Administration, Federal Register, Interim Final Construction Standard, May 4, 1993, p. 26590 (1993).
2. NIOSH, *NIOSH Alert: Request for Assistance in Preventing Lead Poisoning in Construction Workers*, DHHS (NIOSH) Publ. No. 91-116a (NIOSH, Washington, D.C., 1992).
3. S. M. Levin, M. Goldberg, and J. T. Doucette, *Am. J. Ind. Med.* **31**, 303 (1997); see also two related papers on pages 310 and 319.
4. N.-G. Lunstrom, G. Nordberg, V. Englyst, L. Gerhardsson, L. Hagmar, T. Jin, L. Rylander, and S. Wall, *Scand. J. Work. Environ. Health* **23**, 24 (1997).
5. P. J. Seligman, W. E. Halperin, R. J. Mullan, and T. M. Frazier, *Am J. Pub. Health* **76**, 1299 (1986).
6. P. J. Panapek, C. E. Ward, K. M. Gilbert, and S. A. Frangos, *Am. J. Ind. Med.* **21**, 199 (1992).
7. A. Fischbein, *Isr. J. Med. Sci.* **28**, 560 (1992).
8. A. Fischbein, F. Gauer, J. Glick, E. D. Richter, Z. Schlezinger, A. Ben-Tankur, and M. Quastel, *Isr. J. Med. Sci.* **31**, 387 (1995).
9. B. Abudhaise, M. Alzoubi, A. Z. Rabi, and R. M. Alwash, *Int. J. Occupat. Med. And Env. Health* **9**, 323 (1996).
10. H.-W. Kuo, J.-S. Lai, and T.-I. Lin, *AIHA J.* **58**, 29 (1997).
11. H. S. Park, H. J. Yu, and K.-S. Jung, *Clin. Exp. Allergy* **24**, 676 (1994).
12. P. B. Bright, P. S. Burge, S. P. O'Hickey, P. F. G. Gannon, A. S. Roertson, and A. Boran, *Thorax* **52**, 28 (1997).
13. S.-C. Lin, C.-C. Tai, C.-C. Chan, and J.-D. Wang, *Amer. J. Industr. Med.* **26**, 221 (1994).
14. H.-W. Kuo, J.-S. Lai, and T.-I. Lin, *Int. Arch. Occup. Environ. Health* **70**, 272 (1997).
15. L. M. Conroy, R. M. Menezes-Lindsay, P. M. Sullivan, S. Cali, and L. Forst, *Arch. Environ. Health* **51**, 95 (1996).
16. L. M. Conroy, R. M. Menezes-Lindsay, and P. M. Sullivan, *Am. Ind. Hyg. Assoc. J.* **56**, 266 (1995).
17. M. E. Fraser, A. J. R. Hunter, S. D. Davis, L. G. Piper, and K. W. Holtzclaw, "Induced Breakdown Spectroscopy Detection System with Controllable Delay Time", Patent Pending (1999).
18. J. Zynger and S. R. Crouch, *Appl. Spectrosc.* **29**, 244 (1975).
19. L. J. Radziemski and D. A. Cremers, "Spectrochemical Analysis Using Laser Plasma Excitation", in *Laser Induced Plasmas and Applications*, L. J. Radziemski and D. A. Cremers, Eds. (Marcel Dekker, New York, 1989), Chap. 7, p. 295.
20. R. N. Berglund and B. Y. H. Liu, *Anal. Chem.* **7**, 147 (1973).
21. E. R. Kennedy, T. J. Fischbach, R. Song, P. M. Eller, and S. A. Shulman, "Guidelines for Air Sampling and Analytical Method Development and Evaluation", NIOSH Technical Report, Publication No. 95-117 (NIOSH, Washington, D.C., 1995).
22. Performance Testing of Multi-Metal Continuous Emissions Monitors (1996), IS-5128/UC-606 (Ames Laboratory, U.S. Department of Energy, 1997).
23. 1997 Performance Testing of Multi-Metal Continuous Emissions Monitors, DOE/ID-10665 (U.S. Department of Energy, Idaho Operations Office, 1998).
24. A. J. R. Hunter, M. E. Fraser, J. R. Morency, C. L. Senior, T. Panagioutou, and S. J. Davis, "A Spark-Induced Breakdown Spectroscopy Based Continuous Emissions Monitor for Lead and Chromium", in *1997 Performance Testing of Multi-Metal Continuous Emissions Monitors*, DOE/ID-10665 (U.S. Department of Energy, Idaho Operations Office, 1998).
25. G. P. Miller, Z. Zhu, and W. Okhuysen, "Fieldable Air ICP-AES System", in *1997 Performance Testing of Multi-Metal Continuous Emissions Monitors*, DOE/ID-10665 (U.S. Department of Energy, Idaho Operations Office, 1998).
26. M. D. Seltzer, "TraceAIR Multimetal Continuous Emissions Monitor Report and Test Results", in *1997 Performance Testing of Multi-Metal Continuous Emissions Monitors*, DOE/ID-10665 (U.S. Department of Energy, Idaho Operations Office, 1998).
27. D. W. Hahn, K. R. Hencken, H. A. Johnsen, and E. J. Walsh, "Performance Testing of a Laser-Induced Breakdown Spectroscopy (LIBS) Based Continuous Emissions Monitor at the US EPA Rotary Kiln Incinerator Simulator", in *1997 Performance Testing of Multi-Metal Continuous Emissions Monitors*, DOE/ID-10665 (U.S. Department of Energy, Idaho Operations Office, 1998).
28. P. P. Woskov, K. Haddidi, P. Thomas, K. Green, and G. Flores, "Microwave-Plasma Continuous Emissions Monitor", in *1997 Performance Testing of Multi-Metal Continuous Emissions Monitors*, DOE/ID-10665 (U.S. Department of Energy, Idaho Operations Office, 10665 1998).
29. A. J. R. Hunter, J. R. Morency, C. L. Senior, S. J. Davis, and M. E. Fraser, "Continuous Emissions Monitoring Using Spark-induced Breakdown Spectroscopy (SIBS)", accepted for publication in *J. Air and Waste Management Assoc.* (1999).
30. M. E. Fraser, T. Panagioutou, A. J. R. Hunter, E. B. Anderson, S. J. Davis, G. Braybrooke, and K. J. Hay, "Fugitive Emissions Measurements Above a Hard Chrome Plating Tank Using Spark-Induced Breakdown Spectroscopy (SIBS)", accepted for publication in *Plating and Surf. Finishing* (1999).